Shannon Dimensionality of Quantum Channels and Its Application to Photon Entanglement

J. B. Pors,[*] S. S. R. Oemrawsingh,[+] A. Aiello, M. P. van Exter, E. R. Eliel, G. W. 't Hooft, and J. P. Woerdman

Huygens Laboratory, Leiden University, P.O. Box 9504, 2300 RA Leiden, The Netherlands
(Received 14 March 2008; published 18 September 2008)

We introduce the concept of Shannon dimensionality D as a new way to quantify bipartite entanglement as measured in an experiment. This is applied to orbital-angular-momentum entanglement of two photons, using two state analyzers composed of a rotatable angular-sector phase plate that is lens coupled to a single-mode fiber. We can deduce the value of D directly from the observed two-photon coincidence fringe. In our experiment, D varies between 2 and 6, depending on the experimental conditions. We predict how the Shannon dimensionality evolves when the number of angular sectors imprinted in the phase plate is increased and anticipate that $D \simeq 50$ is experimentally within reach.

Photons can be entangled in various degrees of freedom. The most extensively studied variety involves the polarization degrees of freedom, of which there are inherently two per photon. In a typical EPR-Bell-type experiment, the state analyzers are polarizers, and when their relative orientation is scanned, this gives rise to a sinusoidal coincidence fringe [1]. This particular shape is characteristic of the two-dimensional nature of polarization entanglement.

Recently, much attention has been drawn to bipartite entanglement involving more than 2 degrees of freedom. With increasing dimensionality, quantum entanglement becomes correspondingly richer. High-dimensional entanglement is predicted to violate locality more strongly and to show more resilience to noise [2,3]. From an applications perspective, it holds promise for implementing larger alphabets in quantum information, e.g., quantum cryptography [4], and for an increased security against eavesdropping [5]. High-dimensional entanglement can be studied employing the frequency-time [6] or position-momentum degrees of freedom, the latter having been demonstrated for both the transverse linear [7,8] and orbital-angular-momentum degrees of freedom [9,10].

It is crucial to have a quantifier of the dimensionality of entanglement as measured in an experiment [11]. In this Letter, we introduce such a quantifier, using concepts from classical information theory in the spirit of Shannon [12]. We apply these ideas to orbital-angular-momentum entanglement, inserting appropriate angular state analyzers in the beam lines of a parametric down-conversion setup. We have realized a Shannon dimensionality $2 \leq D \leq 6$, and we argue that $D \simeq 50$ is within reach.

In classical information theory [12], the number of independent communication channels of a signal is known as the Shannon number. The signal being the state of a physical system, the Shannon number is also referred to as the number of degrees of freedom, or the number of modes, of that system [13,14]. For example, a signal encoded in the polarization degrees of freedom of a light beam has a Shannon number equal to 2.

When dealing with a bipartite quantum system in an entangled pure state $|\psi\rangle \in \mathcal{K}_A = \mathcal{K}_A \otimes \mathcal{K}_B$, the usual measure of the effective dimensionality of the Hilbert space in which the state lives is given by the Schmidt number K [15]:

$$K = \frac{1}{\mathrm{Tr}_A(\rho_A^2)} = \frac{1}{\mathrm{Tr}_B(\rho_B^2)}. \qquad (1)$$

Here $\rho_A = \mathrm{Tr}_B(|\psi\rangle\langle\psi|)$ and $\rho_B = \mathrm{Tr}_A(|\psi\rangle\langle\psi|)$ are the reduced density matrices representing the states of the two subsystems $A \in \mathcal{K}_A$ and $B \in \mathcal{K}_B$, respectively. Although a system may have infinitely many degrees of freedom, any actual measurement apparatus has effective access only to a finite number of them, say, D. Such a dimensionality D is referred to as the Shannon number of the measurement apparatus.

Consider an experiment measuring correlations between the two subsystems A and B. There are two measuring apparatuses, say, $\mathcal{P}_A(\alpha)$ and $\mathcal{P}_B(\beta)$, interacting with subsystems A and B, respectively, where α and β label possible settings of the two apparatuses. For a given setting $\xi \in \{\alpha, \beta\}$, detector $\mathcal{P}_X(\xi)$ is represented by the projection operator $\hat{\Gamma}(\xi) = |X(\xi)\rangle\langle X(\xi)|$, where $X \in \{A, B\}$ and $|X(\xi)\rangle$ is the state in which the system X is left after measurement.

If a von Neumann-type projective measurement is performed, the set of states $\{|X(\xi)\rangle\}_\xi$ obtained by varying ξ is complete and orthonormal, namely,

$$\langle X(\xi)|X(\xi')\rangle = \delta_{\xi\xi'}, \qquad \sum_\xi \hat{\Gamma}(\xi) = \hat{1}, \qquad (2)$$

where the measurement operators $\hat{\Gamma}(\xi)$ are Hermitian and idempotent. The number of these operators is equal to the dimension of the Hilbert space of the measured quantum system [16]. However, in many situations nonorthogonal measurements are made, and Eqs. (2) do not hold [17]. In this case, the number of projection operators $\hat{\Gamma}(\xi)$ does not

give the dimension of the Hilbert space of the measured system, and a new criterion must be introduced.

Let us therefore consider finite-dimensional systems, say, $\dim(\mathcal{K}_X) = L$, and rewrite Eqs. (2) for the case of nonorthogonal measurements as

$$\langle X(\xi)|X(\xi')\rangle = g_{\xi\xi'}, \qquad \sum_{\xi} \hat{\Gamma}(\xi) = \hat{\gamma}, \qquad (3)$$

where $G = [g_{\xi\xi'}]$ is a matrix of size $L \times L$ and $\hat{\gamma}$ is an Hermitian operator. The eigenvalues γ_l of $\hat{\gamma}$ give the detector's "sensitivity" to the corresponding eigenmodes. In general, a detector will not be equally sensitive to all eigenmodes, and some γ_l are substantially larger than others. The *effective* dimensionality $D \leq L$ of the Hilbert space $\mathcal{D}$ where the *measured* system lives can be quantified as the Hilbert-Schmidt norm of the eigenvalue distribution [18]

$$D \equiv \frac{1}{\mathrm{Tr}(\hat{\gamma}^2)} = \frac{1}{\sum_l \gamma_l^2}. \qquad (4)$$

This dimensionality should be interpreted as the effective Shannon number of information channels [12,13].

The isomorphism of Eqs. (1) and (4) suggests a relation between the Schmidt number K and the Shannon dimensionality D. The nature of such a relation becomes clear if one notes that, since the operators $\hat{\Gamma}(\xi)$ are Hermitian and positive semidefinite, the operator $\hat{\gamma}$ may be interpreted as a density matrix acting in $\mathcal{K}_X$ [19]. Thus, if we think of $\hat{\gamma}$ as a reduced density matrix of a bipartite system, then K and D are formally the same. However, it is important to note that, while K furnishes the dimensionality of the *generated* entanglement, D gives the effective dimensionality of the space $\mathcal{D}$ that can *potentially* be *probed*, and it is a property of the projection apparatus only. The dimensionality of the *measured* entanglement is a joint property of the generated system and analyzers but simply amounts to D as long as $\mathcal{K} \supset \mathcal{D}$.

Next, we apply our formal theory to an experiment on orbital-angular-momentum entanglement of two photons, in order to illustrate how detector characteristics bound the measured entanglement to an effective Shannon dimensionality D, while probing a generated state with Schmidt number $K \gg D$ (and $\mathcal{K} \supset \mathcal{D}$). Our experimental setup is depicted in Fig. 1. Pumping a β-barium borate (BBO) nonlinear crystal with a 150 mW Kr$^+$ laser beam at $\lambda = 413$ nm, we produce spatially entangled photons by means of spontaneous parametric down-conversion. The state that we generate is of the form $|\Psi\rangle = \sum_l \sqrt{\lambda_l} |l\rangle |-l\rangle$, where $|l\rangle$ denotes the orbital-angular-momentum eigenmode of order l: $\langle \phi|l\rangle = \exp(il\phi)/\sqrt{2\pi}$, with ϕ the azimuthal angle [20]. Employing type-I collinear phase matching, we collect the full emission cone, and with the experimental parameters of our setup (beam half-waist at the position of the crystal $w_0 = 250$ μm and crystal length 1 mm), we obtain an azimuthal Schmidt number $K \simeq 31$ [21–23]. The

twin photons are spatially separated by means of a non-polarizing beam splitter.

Each arm of the setup contains an angular state analyzer, composed of an angular phase plate that is lens coupled to a single-mode fiber (see Fig. 1) [24]. The angular phase plates carry a purely azimuthal variation of the optical thickness. As in polarization entanglement [1], the phase plates are rotated around their normals, and the photon coincidence rate is recorded as a function of their independent orientations [10].

The combined detection state of the two angular-phase-plate analyzers, each acting locally, can be expressed as

$$|A(\alpha)\rangle \otimes |B(\beta)\rangle = \left(\sum_l \sqrt{\gamma_l} |l\rangle e^{il\alpha} \right)_A \otimes \left(\sum_l \sqrt{\gamma_l} |l\rangle e^{il\beta} \right)_B, \qquad (5)$$

where α and β denote the orientations of the two phase plates, respectively [25]. The complex expansion coefficients $\sqrt{\gamma_l}$ are fixed by the physical profile of the angular phase plate and obey the normalization condition $\sum_l |\gamma_l| = 1$. In general, the detection state constitutes a nonuniform superposition of orbital-angular-momentum modes. When the angular phase plates are rotated over α or β, all modes in the superposition rephase with respect to each other, yielding a set of detection states of the type Eq. (3). The effective Shannon dimensionality that is so probed is given by Eq. (4). It is the average number of modes captured by an analyzer when its phase plate is rotated over 360°.

As we have recently shown in Ref. [18], the Shannon dimensionality is straightforwardly deduced from the shape of the experimental coincidence curve; it is the inverse of the area underneath the peak-normalized coincidence fringe, obtained when rotating one of the phase plates.
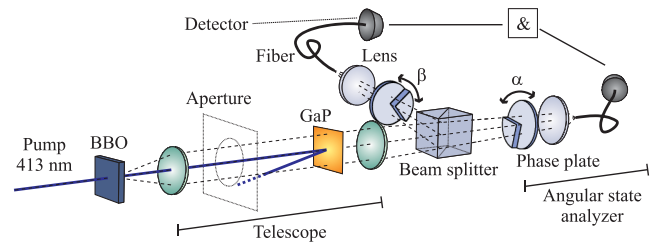

FIG. 1 (color online). Experimental setup. Orbital-angular-momentum entangled photons are emitted at 826 nm by a BBO crystal, cut for type-I collinear phase matching. A thin GaP wafer serves to eliminate the pump beam. The two-photon field can be clipped with an aperture. The twin photons are spatially separated by a beam splitter and imaged on the angular phase plates ($f_2 = 4f_1 = 40$ cm). Just behind the phase plates, the frequency-degenerate photons are selected by interference filters (not shown), centered around 826 nm with a 10 nm width. The phase plates (shown are quarter-sector plates) are oriented at angles α and β, and photon counts are rendered by a coincidence circuit.

In our experiment, we have used angular-sector phase plates; these have a single arc sector, characterized by the angle δ, whose optical thickness is $\lambda/2$ greater than that of the remainder of the plate [24]. The part of the field that crosses this sector thus flips sign. The phase plates are manufactured from fused-quartz plane-parallel plates, having a wedge angle of $0.25''$. They are processed by a combination of photolithography, wet etching, deposition, and lift-off, resulting in a well-defined mesa structure, with a transition region that is typically $20~\mu$m wide. The insets in Fig. 2 show two such plates: a half-sector plate ($\delta = \pi$), consisting of two equal halves that are phase shifted by π, and a quarter-sector plate ($\delta = \pi/2$), having one quadrant π-phase shifted with respect to the remainder of the plate.

For state analyzers that are equipped with such sector phase plates, the Shannon dimensionality is given by [18]

$$D(\delta) = \begin{cases} [1 - 4\frac{\delta}{\pi} + 6(\frac{\delta}{\pi})^2 - \frac{8}{3}(\frac{\delta}{\pi})^3]^{-1}, & \delta \in [0, \pi], \\ D(2\pi - \delta), & \delta \in [\pi, 2\pi]. \end{cases}$$
$$(6)$$

For $\delta = 0$ we find the trivial result $D = 1$; a planar plate

does nothing. For $\delta = \pi$, i.e., a state analyzer equipped with a half-sector plate, we arrive at $D = 3$. For an analyzer equipped with a quarter-sector plate, we find $D = 6$. This is the maximum value for a single angular-sector phase plate. We note that for our setup indeed $K \gg D$.

In the experiment, we scan one angular-sector phase plate over a 360° rotation, the other remaining fixed, and measure the coincidence rate. In terms of Klyshko's picture of advanced waves [26], valid when $K \gg D$, the resulting shape of the coincidence curves can be explained in terms of the mode overlap of the two state analyzers. Figure 2(a) shows experimental results obtained with two half-sector plates ($\delta = \pi$), having a step height of 0.48λ. The data points form a double *parabolic* fringe, consistent with theory (solid curve). The maxima at 0° and 180° are sharply peaked. The zeros of the fringe are very deep, less than 10 counts per 10 seconds. The maximum coincidence rate is of the order of 6.5×10^3 per 10 seconds, compared to 10^5 single counts. We verified that the coincidence rate depends on the *relative* orientation between the two phase plates only, the fringe visibility being >99% for all cases studied. This basis independence is the key aspect of quantum entanglement. From the area underneath the data, we deduce the experimental value $D = 3.0$. Note that a parabolic fringe was also reported in Ref. [10], obtained with noninteger spiral phase plates. We conclude that also in that case $D = 3$.

An aperture, positioned inside the telescope, allows us to control the number of detected modes (see Fig. 1). Because of the antisymmetric profile of the half-sector plate, the detection state contains only odd expansion terms [see Eq. (5)] in a fashion $\gamma_l = \gamma_{-l}$. When the aperture size is reduced, higher-order orbital-angular-momentum modes are cut off so that, eventually, only the modes $l = 1$ and $l = -1$ survive. We then expect a sinusoidal fringe, analogous to two-dimensional polarization entanglement [1]. In the experiment, we observe that the coincidence curve is gradually transformed from parabolic to sinusoidal when the aperture gets smaller. Using an aperture of $600~\mu$m diameter, we are in an intermediate regime (squares, $D = 2.1$), while using a $400~\mu$m diaphragm yields a curve that resembles a sine very well (triangles, $D = 2.0$). The dashed and dotted curve are theoretical predictions.

To achieve $D = 6$, we use two quarter-sector plates ($\delta = \pi/2$), carrying an edge discontinuity deviating less than 3% from $\lambda/2$. The circles in Fig. 2(b) show our experimental results, revealing a coincidence curve which is parabolic for $|\alpha - \beta| \leq 90°$ and equal to zero otherwise, in agreement with theory (solid curve). We find $D = 5.8$, in very good agreement with the expected value of 6 mentioned above.

The maximum value of the Shannon dimensionality that can be achieved with a phase plate having but a single sector is $D = 6$. Can one reach higher values of D by using plates with more sectors? To answer this question, we consider plates with N sectors that are phase shifted by π with respect to interjacent regions. For each choice of
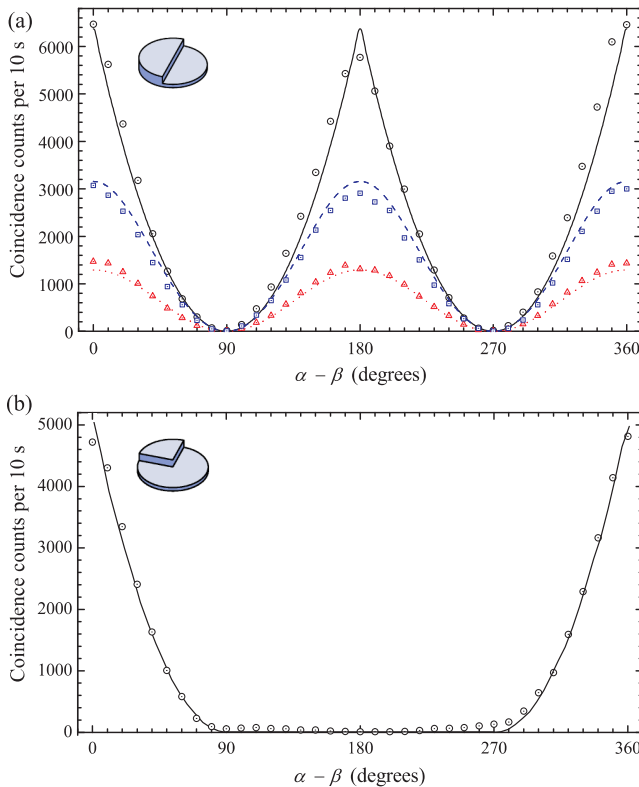
FIG. 2 (color online).   Coincidence count rate vs the relative orientation of the two state analyzers. Points denote experimental data; curves are theoretical predictions. (a) Half-sector plate. The parabolic fringe (circles) is a signature of a dimensionality larger than 2: We find $D = 3.0$. Truncating the number of modes, by closing the aperture, gradually reduces the parabola into a sine of dimensionality 2.0 (triangles). (b) Quarter-sector plate. The piecewise parabolic fringe yields an experimental dimensionality of 5.8 (circles), where theory predicts $D = 6$.
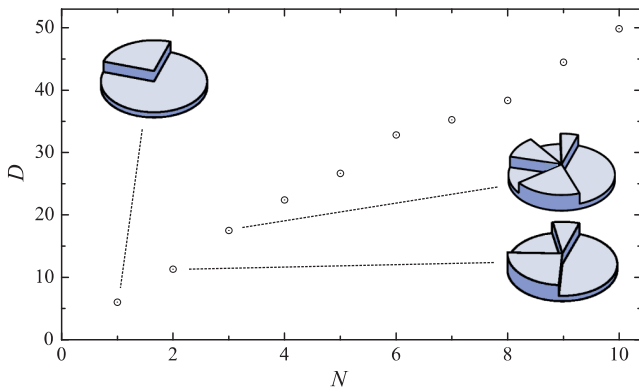
FIG. 3 (color online).   Maximum dimensionality that can be accessed with sector phase plates having $2N$ angular sectors alternatingly phase shifted by π. The insets show the optimized plates for $N = 1$, $N = 2$, and $N = 3$.

sector angles, we calculate the expansion coefficients $\{\sqrt{\gamma_l}\}$ and, subsequently, D [see Eqs. (4) and (5)]. Next, we maximize D by adjusting the sector angles using a Monte Carlo random-search algorithm. The result is plotted in Fig. 3, showing a graph of the maximum value of D versus the number of mesas N. For 10 such sectors, we find $D = 49.9$. The insets show the optimal phase plates for $N = 1$ (quarter-sector plate), $N = 2$, and $N = 3$.

In conclusion, we have introduced the effective Shannon dimensionality as a novel quantifier of entanglement as measured in an actual experiment. We have demonstrated its significance to the case of two-photon orbital-angular-momentum entanglement. Using angular-sector phase plates, we have achieved Shannon dimensionalities up to $D = 6$. We anticipate that it is feasible to probe dimensionalities as high as 50, using multisector phase plates. These can be manufactured by means of photo- or e-beam lithography as in diffractive-optics technology. Alternatively, the use of adaptive optical devices, such as spatial light modulators or micromirror arrays, seems promising, particularly because of their versatility with regard to plate patterns. However, the ultimate limit to the Shannon dimensionality is constrained by the angular Schmidt number of the source; using periodically poled crystals, $K \sim 100$ is viable for realistic values of pump-beam waist and crystal length, without loss of count rates [27].

*pors@molphys.leidenuniv.nl
+Present address: Department of Physics, University of California, Santa Barbara, CA 93106, USA.

[1] A. Aspect, P. Grangier, and G. Roger, Phys. Rev. Lett. **47**, 460 (1981).

[2] D. Collins, N. Gisin, N. Linden, S. Massar, and S. Popescu, Phys. Rev. Lett. **88**, 040404 (2002).

[3] D. Kaszlikowski, P. Gnaciński, M. Żukowski, W. Miklaszewski, and A. Zeilinger, Phys. Rev. Lett. **85**, 4418 (2000).

[4] H. Bechmann-Pasquinucci and W. Tittel, Phys. Rev. A **61**, 062308 (2000).

[5] L. Zhang, C. Silberhorn, and I. A. Walmsley, Phys. Rev. Lett. **100**, 110504 (2008).

[6] H. de Riedmatten, I. Marcikic, H. Zbinden, and N. Gisin, Quantum Inf. Comput. **2**, 425 (2002).

[7] L. Neves, G. Lima, J. G. Aguirre Gómez, C. H. Monken, C. Saavedra, and S. Pádua, Phys. Rev. Lett. **94**, 100501 (2005).

[8] M. N. O'Sullivan-Hale, I. A. Khan, R. W. Boyd, and J. C. Howell, Phys. Rev. Lett. **94**, 220501 (2005).

[9] A. Mair, G. W. A. Vaziri, and A. Zeilinger, Nature (London) **412**, 313 (2001).

[10] S. S. R. Oemrawsingh, X. Ma, D. Voigt, A. Aiello, E. R. Eliel, G. W. 't Hooft, and J. P. Woerdman, Phys. Rev. Lett. **95**, 240501 (2005).

[11] N. Brunner, S. Pironio, A. Acín, N. Gisin, A. A. Méthot, and V. Scarani, Phys. Rev. Lett. **100**, 210503 (2008).

[12] C. E. Shannon and W. Weaver, *The Mathematical Theory of Communication* (University of Illinois Press, New York, 1949).

[13] G. Toraldo di Francia, J. Opt. Soc. Am. **59**, 799 (1969).

[14] F. Gori and G. Guattari, Opt. Commun. **7**, 163 (1973).

[15] M. U. Karelin, Opt. Spectrosc. **103**, 193 (2007).

[16] H. E. Brandt, Am. J. Phys. **67**, 434 (1999).

[17] R. T. Thew, K. Nemoto, A. G. White, and W. J. Munro, Phys. Rev. A **66**, 012303 (2002).

[18] J. B. Pors, A. Aiello, S. S. R. Oemrawsingh, M. P. van Exter, E. R. Eliel, and J. P. Woerdman, Phys. Rev. A **77**, 033845 (2008).

[19] I. Bengtsson and K. Życzkowski, *Geometry of Quantum States: An Introduction to Quantum Entanglement* (Cambridge University Press, Cambridge, England, 2006).

[20] S. P. Walborn, A. N. de Oliveira, R. S. Thebaldi, and C. H. Monken, Phys. Rev. A **69**, 023811 (2004).

[21] C. K. Law and J. H. Eberly, Phys. Rev. Lett. **92**, 127903 (2004).

[22] M. P. van Exter, A. Aiello, S. S. R. Oemrawsingh, G. Nienhuis, and J. P. Woerdman, Phys. Rev. A **74**, 012309 (2006).

[23] M. P. van Exter, P. S. K. Lee, S. Doesburg, and J. P. Woerdman, Opt. Express **15**, 6431 (2007).

[24] S. S. R. Oemrawsingh, J. A. de Jong, X. Ma, A. Aiello, E. R. Eliel, G. W. 't Hooft, and J. P. Woerdman, Phys. Rev. A **73**, 032339 (2006).

[25] The set of orbital-angular-momentum eigenmodes constitutes the appropriate basis to expand the detection state, for these modes are eigenfunctions of rotation over α, and the set contains the fiber mode $l = 0$.

[26] A. V. Belinskii and D. N. Klyshko, Zh. Eksp. Teor. Fiz. **105**, 487 (1994) [JETP **78**, 259 (1994)].

[27] M. Fiorentino, S. M. Spillane, R. G. Beausoleil, T. D. Roberts, P. Battle, and M. W. Munro, Opt. Express **15**, 7479 (2007).